A novel SAR imaging method under geographical coordinates

LI Yanghuan, JIN Tian, SONG Qian, ZHOU Zhimin

Ultra-Wide Band Radar Laboratory College of Electronic Science and Engineering, National University of Defense Technology, Hunan Changsha 410073, *China*

Abstract: Traditional airborne SAR (Synthetic Aperture Radar) makes use of the GPS/INS to compensate the platform motion error to acquire high resolution images. GPS data with geographical coordinates (consists of longitude, latitude and height) is converted to a local Cartesian coordinates, under which raw radar data is processed with some imaging and motion compensation algorithms to create an image with the local coordinates. However, it is not easy to be understood for other departments who need an image located by geographical coordinates. This paper presents a novel SAR imaging algorithm derived from Back-Projection that can be processed directly under the geographical coordinates and avoid coordinates transformation. Each pixel of the image obtained via this algorithm is located with geographical coordinates, which is convenient to be applied by the intelligence or other survey departments. Images obtained under geographical coordinates by this algorithm are as clear as traditional algorithms that been proved by simulations and an outside experiment.

Key words: Synthetic Aperture Radar, motion compensation, geographical coordinates, coordinates transformation, elevation calibration

CLC number: TP722.6 **Document code:** A

Citation format: Li Y H, Jin T, Song Q and Zhou Z M. 2011. A novel SAR imaging method under geographical coordinates. *Journal of Remote Sensing*, **15**(4): 680–686

1 INTRODUCTION

Nowadays, Synthetic Aperture Radar (SAR) images are both used in military field and in other civil life such as nature disaster forecasting, geologic reconnaissance, geologic charting, polar region surveillance, forest exploitation programming (Luojus, *et al.*, 2009; Zhang, *et al.*, 2009). However, the images obtained by common SAR algorithms can not be applied directly as they are not located with global position information, in other words, there are variations between the image and ground coordinates. The radiometric slope of the image brought by the spherical fluctuating ground surface should be modified firstly (Ulander, 1996). The geocoding procedure is following, by which each pixel will get a pair of geographical coordinates (He & Wang, 2006) . Thereafter, any targets interested in the SAR image could be located by their longitudes and latitudes (Yu, *et al.*, 2007).

Airborne SAR makes use of GPS/INS to get real-time position information of the platform to compensate the motion error that is presented (Kirk, 1975). RTK (Real-Time Kinematic) GPS could produce position information whose error is less than 3 cm while updating rate to 50 Hz (Arai & Shikada, 2001; Earle, *et al.*, 2005; Yang & Lo, 2000). Due to its high updating rate and no authorization restriction, it could replace GPS/INS system in some missions when the task scope is not too large as to overrun the RTK's constraint. The UAV (Unmanned Aircraft Vehicle) SAR, has small observation area, small activity scope and it is appropriated to be equipped RTK GPS. Traditional SAR imaging algorithms and motion compensation algorithms are presented under Cartesian coordinates, accordingly, the geographical coordinates produced by RTK GPS should be transformed to Cartesian coordinates in advance. Finally, we can obtain an image under the local Cartesian coordinates and the targets could be relocated with the geographical coordinates.

There are two defects about traditional SAR algorithms. Firstly, traditional transformation between coordinates needs precise absolute coordinates. RTK GPS needs control points to calibrate the base station, only by which precise absolute coordinates could be obtained. But it is difficult to acquire the control points sometimes. Secondly, the two transform procedures will complicate the SAR processing procedure and introduce new errors. We are looking forward to finding a way to imaging directly under the geographical coordinates and there are seldom references we could find that mention any algorithm for imaging in this way.

This paper presents a novel imaging algorithm that developed from the Back-Projection (BP) algorithm (Rau & McClellan, 2000).

Received: 2010-04-08; **Accepted**: 2010-10-10

Foundation: the National Natural Science Foundation of China (No. 60972121)

First author biography: LI Yanghuan (1982—), male, now he is a doctorate candidates in National University of Defense Technology, China. His research interests are radar imaging, motion compensation, circular synthetic aperture radar and 3-D SAR imaging. E-mail: poptopli@163.com

Corresponding author: JIN Tian (1980—), he is an adjunct professor working in College of Electronic Science and Engineering, National University of Defense Technology. His doctor dissertation has been chosen into one hundred excellent dissertation of China in 2009. He is studying for target shallow buried imaging and detection. E-mail: tianjin@nudt.edu.cn

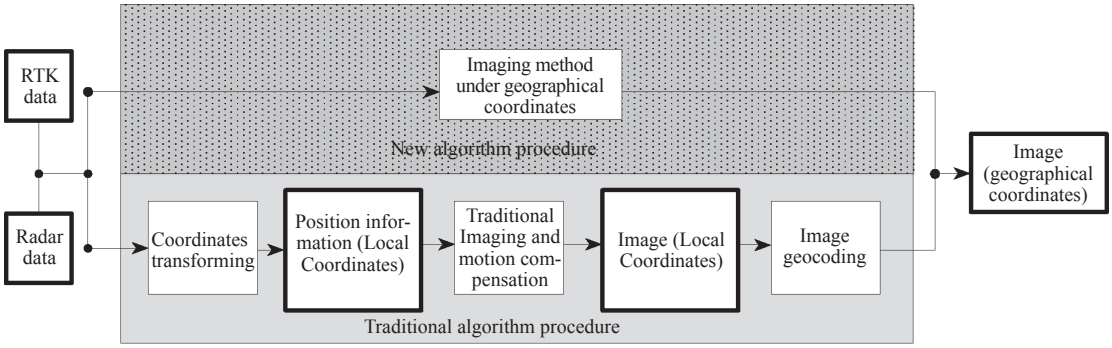

Fig. 1 The procedure of traditional and the new algorithm in this study

In this algorithm the RTK GPS data is introduced directly into imaging process, and then an image under geographical coordinates is obtained, avoiding the two transform procedures. The relationship between this algorithm and traditional algorithm is shown in Fig. 1. In this paper the radar is supposed to work on the strip-map SAR mode and the track of the airborne radar is supposed as linear with some intense vibrations in the slant range direction. The UAV's observation area is relatively small so that the spherical ground surface could be approximated to a plane and the radio slope correcting is not needed here. The RTK GPS could only supply the relative coordinates without any control points. The reason for this algorithm can acquire an image with high quality is because only relative distance is needed.

2 MOTION COMPENSATION

Motion compensation is the key step in an airborne SAR imaging procedure. Time domain algorithm could realize this just as the BP algorithm (Rau and McClellan, 2000), which could be presented by

$$f(x,r)=\int_{-\infty}^{\infty}\int_{-\infty}^{\infty}\frac{t^2}{r}\mathrm{d}(\hat{x},t)w\left(\frac{\hat{x}-x}{r}\right)\delta\left(t-\frac{2R(x,r,x)}{c}\right)\mathrm{d}\hat{x}\mathrm{d}t \quad (1)$$

where x, r denote the azimuth and range coordinates of the image pixel; $f(x, r)$ is the image pixel value; t is the fast time; $\hat{x}$ is radar position corresponding to each echo column; $\mathrm{d}(\hat{x}, t)$ is the echo matrix which has been range compressed; $w(\cdot)$ is antenna shape function; $\delta(\cdot)$ is the unit impulse function; $R(x, r, \hat{x})$ is the distance between image pixel (x, r) and radar position $\hat{x}$. Note that the position of radar and image will both be denoted by geographical coordinates as (b, l, h). The radar position (b_k, l_k, h_k), which is offered by the RTK GPS, denotes the place where it acquires the k_{th} column echo. (b', l', h') is the image pixel position $\boldsymbol{p}'$. So Eq.(1) could be written as

$$f(b',l',h')=\sum_k\int_{-\infty}^{\infty}\frac{t^2}{R_s(b',l',h')}\mathrm{d}_k(t)w'(k,b',l',h')\cdot\delta\left(t-\frac{2R(k,b',l',h')}{c}\right)\mathrm{d}t \quad (2)$$

$$f(\boldsymbol{p}')=\sum_k\int_{-\infty}^{\infty}\frac{t^2}{R_s(\boldsymbol{p}')}d_k(t)w'(k,\boldsymbol{p}')\delta\left(t-\frac{2R_k(\boldsymbol{p}')}{c}\right)\mathrm{d}t \quad (3)$$

where $w'(k, \boldsymbol{p}') = w\left(\frac{\sqrt{R_k^2(\boldsymbol{p}')-R_s^2(\boldsymbol{p}')}}{R_s(\boldsymbol{p}')}\right)$, $R_s(\boldsymbol{p}')$ is the nearest distance between the track line and pixel $\boldsymbol{p}'$. It is convenient to obtain the whole image by Eq.(3) when $R_s(\boldsymbol{p}')$ and $R_k(\boldsymbol{p}')$ are both known for each $\boldsymbol{p}'$. $R_k(\boldsymbol{p}')$ varies when the radar is moving, and it denotes the distance between point $\boldsymbol{p}'$ and the radar position when it transmitting the k_{th} microwave. The motion features are included in $R_k(\boldsymbol{p}')$ as well, which can compensate the motion error.

3 IMAGING UNDER GEOGRAPHIC COORDINATES

There are many methods to calculate the distance $R(k, p')$ between two points using their geographic coordinates (Sansosti, *et al.* 1997). One of them is presented as Eq.(4):

$$f_{dis}(\boldsymbol{p}_1,\boldsymbol{p}_2)=\sqrt{[(l_2-l_1)e_c\cos b_1]^2+[(b_2-b_1)e_c]^2}$$
$$e_c=R_{ep}+(R_{ep}-R_{ee})\cdot(1-2l_1/\pi) \quad (4)$$

where R_{ep} is the polar radius; R_{ee} is the equatorial radius of the earth; (b_1,l_1) is the latitude and the longitude of point $\boldsymbol{p}_1$, and (b_2,l_2) denotes the other point. The place in this study is near ($N$26°,$E$112°), so we set the beginning point as (b_1,l_1), where b_1=$N$26°, l_1=$E$112°, then calculate the distance variation with the longitude and the altitude changing. The result is shown in Fig. 2, x axis shows Δb and Δl that are the variation of altitude and longitude, respectively, y axis shows the distance as $R(\Delta b)$=$f_{dis}((b_1,l_1),(b_1+\Delta b_1,l_1))$ and $\mathrm{R}(\Delta l)$= $f_{dis}((b_1,l_1),(b_1,l_1+\Delta l_1))$. $R(\Delta b)$ and $\mathrm{R}(\Delta l)$ are illustrated separately by dots. Linear lines that almost superpose $R(\Delta b)$ and $\mathrm{R}(\Delta l)$ are drawn by lines. With this, it is easy to find that $R(\Delta b)$ and $\mathrm{R}(\Delta l)$ are very approximate to the linear functions within 100 km. Besides, the longitude lines are perpendicular to the latitude lines. Therefore, in our task the longitude latitude grid could be supposed to a special rectangular coordinates system. The axes are the longitude and latitude that have been divided into equidistant units separately with different scales. The height of the aircraft is supposed to be a constant during the flight, the ideal track of the airplane is expressed by a linear equation b=k_1l+k_2, where b and l are the latitude and longitude of the airplane, k_1 and k_2 are the coefficient to be sought by Least Squares Method (LSM) through the actual points (b_k, l_k) known by the RTK system according to Eq.(5). As shown in Fig. 3, line a_1 is the actual track, a_2 denotes the ideal track.

$$\sum_k(k_1l_k+k_2-b_k)^2\to\min \quad (5)$$

We can define one axis of the coordinates as the flight direction under the local Cartesian coordinates easily, then the observation area becomes a strip region along the track. The area could be expressed by $[x_{\min}, x_{\max}]$ and $[y_{\min}, y_{\max}]$. However, it is difficult to do the same work under the geographic coordinates because

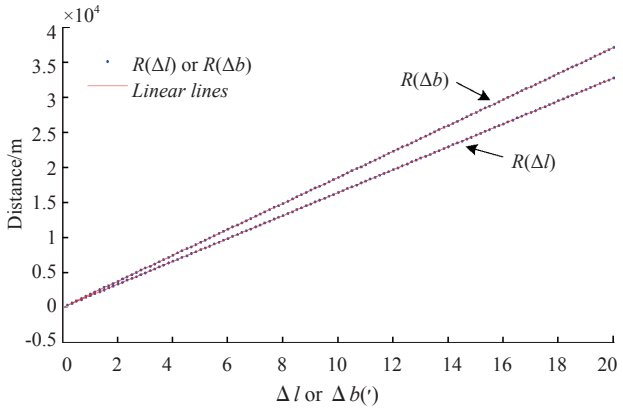

Fig. 2 The distance variation with Δb and Δl. Dots lines denote $R(\Delta b)$ and $R(\Delta l)$; Linear lines that approximating to $R(\Delta b)$ and $R(\Delta l)$.

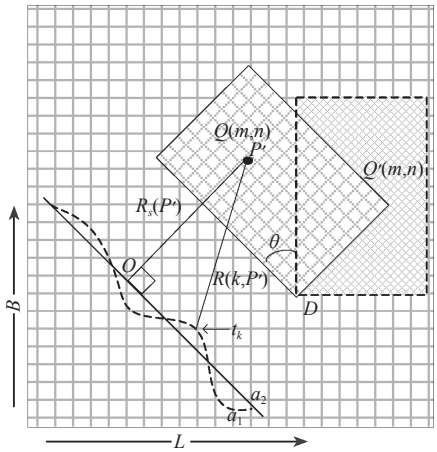

Fig. 3 Imaging under geographical coordinates

the flight track will not always be paralleled to either longitude or latitude lines. To find a way to express the observation area is one important step of this algorithm. A matrix $Q_{M\times N}$ whose cell $(b^Q_{m,n}, l^Q_{m,n})$ is of geographic coordinates is needed to denote the imaging area. The imaging process should focus on the interested area rather than a great deal of trashy area, by which the imaging efficiency will increase substantially. Firstly, determine the irradiated area's minimum distance d_n and maximum distance d_f away from the track's projection on the ground, and the area's length d_0 along cross range direction. These parameters can be obtained by the known beam angle, the slant angle and the flight height. Define the mean value of the serial track coordinates as $(\bar{b},\bar{l})$, and calculate Δr_L that is the distance between two points near $(\bar{b},\bar{l})$ with 1" longitude variation. Use the same method to calculate Δr_B. Follow this, calculate the position D $(b_D, l_D)$by d_n and the track coordinates as shown in Fig. 3. A dashed frame whose one vertex is D is shown in Fig. 3, and its longitude range is $[l_D, l_D+(d_f-d_n)/\Delta r_L]$, latitude range is $[b_D, b_D+d_0/\Delta r_B]$. It is possible to divide the rectangular Q' into a grid $(b^Q_{m,n}, l^Q_{m,n})$ by the aimed resolution Δr_L and Δr_B. Then the grid $(b^Q_{m,n}, l^Q_{m,n})$ could be acquired by shifting and rotating the coordinates according to

$$\begin{cases} b^Q_{m,n} = (b^{Q'}_{m,n} - b_D)\cos\theta + (l^{Q'}_{m,n} - l_D)\sin\theta + b_D \\ l^Q_{m,n} = -(b^{Q'}_{m,n} - b_D)\sin\theta + (l^{Q'}_{m,n} - l_D)\cos\theta + l_D \end{cases} \tag{6}$$

where θ is determined by the flight track, *i.e.* θ=arctan $k_1-\frac{\pi}{2}$.

Given $A = \begin{bmatrix} \cos\theta, \sin\theta \\ -\sin\theta, \cos\theta \end{bmatrix}$, $T_{m,n} = \begin{bmatrix} b^Q_{m,n} \\ l^Q_{m,n} \end{bmatrix}$, $T^D_{m,n} = \begin{bmatrix} b_D\,|_{M\times N} \\ l_D\,|_{M\times N} \end{bmatrix}$,

$T'_{m,n} = \begin{bmatrix} b^{Q'}_{m,n} \\ l^{Q'}_{m,n} \end{bmatrix}$, Eq.(6) could be written to Eq.(7)

$$T_{m,n} = A\times(T'_{m,n} - T^D_{m,n}) + T^D_{m,n} \tag{7}$$

According to Eq.(3), the pixel value of each cell $(b^Q_{m,n}, l^Q_{m,n})$ of $Q_{M\times N}$ can be calculated one by one when the height of each point is supposed to a same value h_0. Obviously, the computation pressure is as heavy as the BP algorithm. The total operation count is $OP \propto L\times M\times N$, where L is the aperture length, $M\times N$ is final size of the image. So the dividing method introduced above, by which the imaging area becomes smaller, is necessary to increase the computing speed. Please note that $R_k(\boldsymbol{p}')$ should be calculated first to get the minimum value $R_s(\boldsymbol{p}')$.

$$R_s(\boldsymbol{p}') = \min_k\{R(k, \boldsymbol{p}')\} \tag{8}$$

A hypothesis in the forward process is that the area to be imaged is of the same height, which means the ground could be approximated to an ideal plane. It will be illconsidered in a mountainous region or a ground with intense height variation (Kwok, *et al.*, 1987; Sansosti, *et al.*, 1997), and the migration between image and ground coordinates should be corrected (Caves, *et al.,* 1991; Hong, *et al.*, 2004; Noack, *et al.*, 1987). If the Digital Elevation Model (DEM) of the imaging area is known in advance, it is easy to acquire the image by replacing h_0 with h=$g(b,l)$ according to Eq.(3). If the DEM, flight parameters and the SAR image with geographical coordinates are known except for raw echo data, an additional step to correct the image called elevation calibration will be needed. This procedure is presented as following: point A's actual geographic coordinates (b_A,l_A,h_A) is known and its coordinates (b'_A,l'_A,h'_A) in SAR image is to be solved. After that the pixel value of A could be obtained by interpolating the known image. It is actually a projection procedure from true topographic data to SAR image. The SAR image only has region and azimuth information (Eineder & Adam, 2005), so the projection is feasible because it is from high dimension to low dimension.

Fig. 4(a) is the view along the flight direction, and Fig. 4 (b) is the view from sky to ground. In Fig. 4(a), the dashed line denotes the ground surface, O is the intersection of the paper plane and the flight track that is perpendicular to the paper plane, the horizontal axis denotes the plane where the SAR image is located at, the vertical axis denotes the height. For an actual point A with a h_A vertical distance from the image height, its projection to the image will be A'. Point O is equidistant from A and A', and the location error is ΔR_A that is made use of to correct the geographic coordinates. It is obvious that

$$\Delta R_A = \sqrt{R_A^2 - h_A^2} - \sqrt{R_A^2 - (h_0 - h_A)^2} \tag{9}$$

$$\begin{cases} l'_A = l_A + \Delta L_A = l_A + \Delta R_A\cdot\cos\theta'/\Delta r_L \\ b'_A = b_A + \Delta B_A = b_A + \Delta R_A\cdot\sin\theta'/\Delta r_B \end{cases} \tag{10}$$

where ΔL_A and ΔL_B are the coordinates corrections that from $(b_A,$

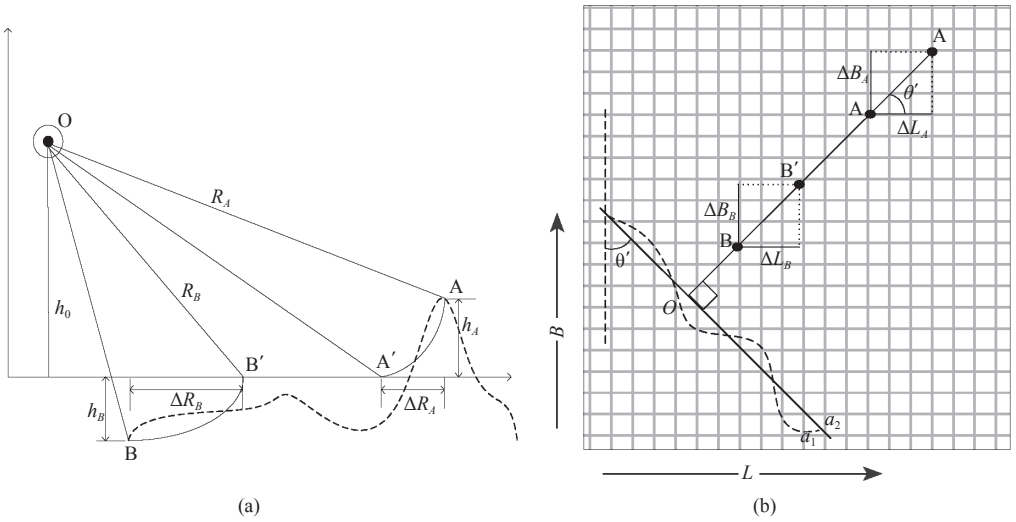

Fig. 4 Elevation calibration for SAR image
(a)the view along the flight direction; (b) the view from sky to ground

l_A, h_A) to (b'_A, l'_A, h'_A), θ' denotes the flight direction under the coordinates whose axis steps at a fixed distance, yet θ defined above is under the coordinates whose axis steps at a fixed longitude or latitude. $\cos\theta'$ and $\sin\theta'$ in (10) could be solved by

$$\begin{cases} \cos\theta' \approx \dfrac{R_L}{R} = \dfrac{f_{dis}(\boldsymbol{p}_o, \boldsymbol{p}_{l1}) + f_{dis}(\boldsymbol{p}_o, \boldsymbol{p}_{l2})}{f_{dis}(\boldsymbol{p}_o, \boldsymbol{p}_{\text{start}}) + f_{dis}(\boldsymbol{p}_o, \boldsymbol{p}_{\text{end}})} \\ \sin\theta' \approx \dfrac{R_B}{R} = \dfrac{f_{dis}(\boldsymbol{p}_o, \boldsymbol{p}_{b1}) + f_{dis}(\boldsymbol{p}_o, \boldsymbol{p}_{b2})}{f_{dis}(\boldsymbol{p}_o, \boldsymbol{p}_{\text{start}}) + f_{dis}(\boldsymbol{p}_o, \boldsymbol{p}_{\text{end}})} \end{cases} \tag{11}$$

where $\boldsymbol{p}_0=(\bar{b}, \bar{l})$ is mean value of the track coordinates sequence, $\boldsymbol{p}_{\text{start}}=(b_1, l_1)$ is start point of the track, $\boldsymbol{p}_{\text{end}}=(b_2, l_2)$ is end point of the track, and $\boldsymbol{p}_{l1}=(\bar{b}, l_1)$, $\boldsymbol{p}_{l2}=(\bar{b}, l_2)$, $\boldsymbol{p}_{b1}=(b_1, \bar{l})$, $\boldsymbol{p}_{b2}=(b_2, \bar{l})$. As shown in Fig. 4(a), the point B is h_B below the imaging plane, so the h_B will be minus causing ΔR_B minus accordingly. If the DEM data is of low resolution, we should interpolate it to high resolution first. After processing all the points in the true geographical map, we can obtain a corrected and geocoded SAR image. It should be noted that, the whole imaging process does not need any absolute coordinates, and it only needs precise relative coordinates. It is known that RTK GPS could supply precise relative coordinates without any control points. That means the coordinates of any points may not be absolutely precise in the global geographical coordinates, but the distance and angle relations among the points will be precise.

4 EXPERIMENTS

A simulation of four point targets set as " T " has been made, and the distance between two neighboring targets is about 2 m. The airplane flights along b=l−84 under the geographic coordinates, where b denotes the latitude and l denotes the longitude, the nearest distance between the track and the center point of the "T" is about 200 m. The altitude of the ground is 50 and the flight altitude is 100 m. The radar signal is single cycle impulse with a center frequency of 500 MHz. If we divide the imaging area according to the longitude and the latitude directly like [$b_{\min}$, $b_{\max}$] and [$l_{\min}$, $l_{\max}$] , the imaging result is shown in Fig. 5(a). The x axis represents longitude within a range of [111.998947º, 111.999047º], and this range minus 111.99º forms the final range. The y axis denotes latitude within range of [28.001946º, 28.002046º], and this range minus 28º forms the final range. In this experiment, certain areas are useless and the nonirradiated areas can lead to a waste of computation. Actually the valid observation area is the region inside the dashed rectangle in Fig. 5(a). If we divide the imaging area along the flight track according to the steps presented in this paper, we could get the valid rectangular area, which is shown in Fig. 5(b). In this image, the axis does not denote the longitude or latitude anymore, because none rows of the pixels share the same latitude and none columns of the pixels share the same longitude. Therefore, the length and width of the image could be scaled, with each pixel having separate geographic coordinates. There will not be useless area imaged in Fig. 5(b), and the computation efficiency can be increased. Then the ground surface is supposed fluctuating by setting the targets' altitude with 1—2 m variations, and the common imaging result is shown in Fig. 5(c). The " T " has been distorted because of the variations in targets' altitude. It has been found that the true position of the target may no longer be a highlight point in the image. Now the elevation calibration method presented in this paper will be accomplished. Take the bottom target for example, it is located at (28.00201º,111.99899º) and −2 m below the original image altitude. Calculate Eq.(9) to get ΔR_A=−0.43668, and get $\sin\theta'$=−0.7479, $\cos\theta'$=0.6638 by Eq. (11). Then the corrected coordinates of the target in the image is obtained as (28.0020123º,111.998987º), which is the exact position of the bottom highlighted point in the image. If we know all the altitudes of points, a corrected and geocoded SAR image will be acquired.

In the outside experiment, an impulse radar is set about 4 m high on a vehicle radiating side of the forward direction. This vehicle is moving along a curve approximating to a straight line to simulate the airplane's flying condition. Five small trihedral angles are set as "┼" on the flat ground as shown in Fig. 6(d). Due to the flat ground, the elevation calibration is not necessary. An area of about 4 m×5 m including these trihedral angles is to be imaged, and the result is shown in Fig. 6(a). We use traditional back-projection

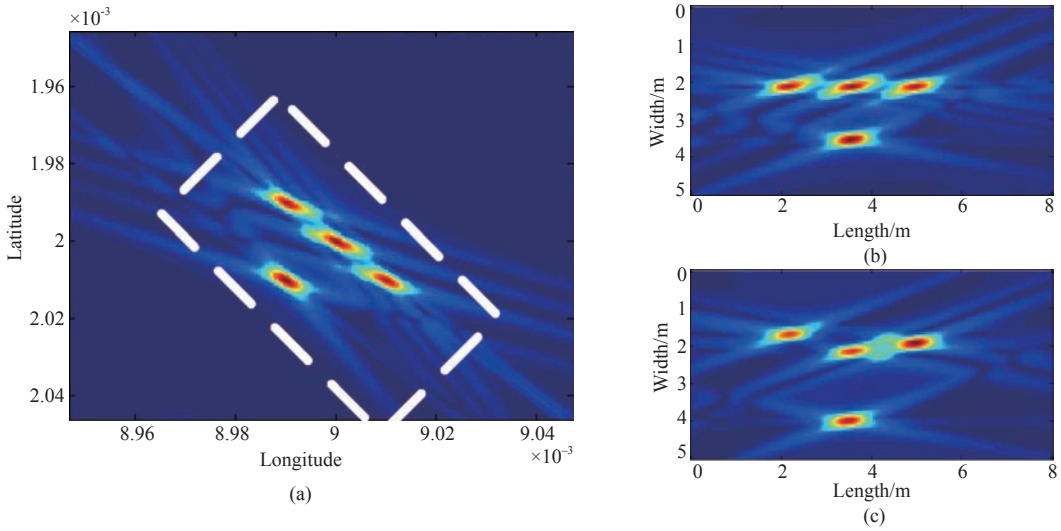

Fig. 5 “ T ” targets imaging results
(a) divide imaging area according to the longitudes and latitudes; (b) divide the imaging area according to the steps presented in this paper; (c) heights variations supposed among the targets

algorithm under local Cartesian coordinates to form an image that is shown in Fig. 6(b). Obviously, the coordinate transformation is inevitable, but there is no prior known control point. So the error introduced by the coordinate transformation causes the low precision of imaging. Reconnaissance by UAV for some special kind of targets could produce a series of images like Fig. 6(a), and then make use of them to form reliable map information. Take the map within [E112º51'58.615", E112º51'58916"] and [N28º13'01.873", N28º13'02.533"] for example, we could detect the targets' pixels first and put them on the map by its geographical coordinates which is shown in Fig. 6(c). Reconnaissance could be accomplished by a multi-mission for each mission finishing a part of the map. Then an exhaustive map containing these special targets will be accomplished.

Table 1 Targets coordinates

Target	New Algorithm		Traditional Algorithm		Distance /m
	Longitude	Latitude	Longitude	Latitude	
①	51'58.7946	13'02.1868	51'58.7952	13'02.1904	0.1120
②	51'58.8370	13'02.2174	51'58.8371	13'02.2196	0.0678
③	51'58.8000	13'02.2192	51'58.8000	13'02.2210	0.0554
④	51'58.7622	13'02.2216	51'58.7622	13'02.2242	0.0800
⑤	51'58.8022	13'02.2521	51'58.8034	13'02.2539	0.0644

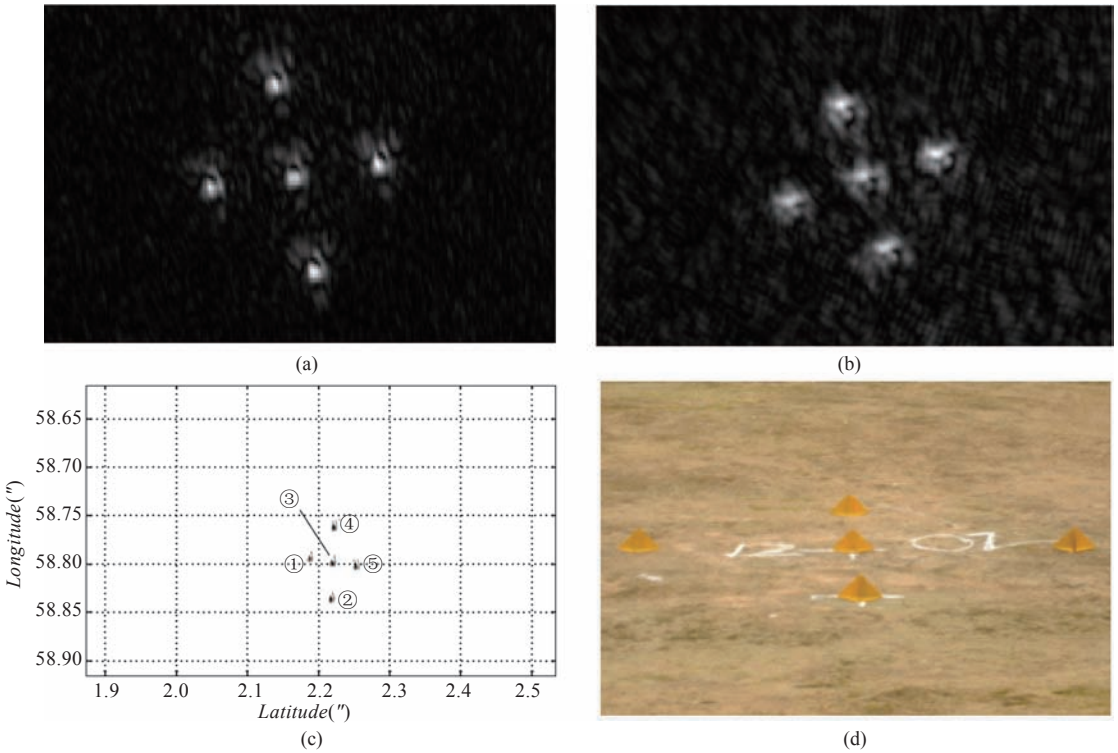

Fig. 6 The imaging results of an experimental data

In order to compare the location precisions between the new algorithm and the traditional algorithm, the targets coordinates located by both two algorithms are shown in Table 1. Targets' distances between positions located by different algorithms of the same target are also included in Table 1. Though we do not have the true absolute coordinates of the targets, distance between target ① and target ③ was set as 1 meter before. The distance of target ②③, ④③, ⑤③ are also set 1 m. These distances are calculated and are shown in Table 2, from which we can find that the new algorithm produces better results than the traditional algorithm. The error of the distance is near 3 cm which is about the utmost measurable precision of RTK GPS. So the algorithm presented in this paper does not increase the location error.

Table 2 Targets distances comparison

Targets	New Algorithm /m	Traditional Algorithm/m	True distance /m	Whose Error is small
①③	1.0082	0.9511	1	N
②③	1.0104	1.0126	1	N
④③	1.0334	1.0354	1	N
⑤③	1.0146	1.0146	1	N/T

5 CONCLUSION

A novel SAR imaging algorithm that introduces the RTK GPS data to compensate the platform motion error and to geocode the image under geographical coordinates is presented in this paper. This algorithm avoids additional coordinate transformation, which will simplify the procedure of airborne SAR reconnaissance. Both imaging area dividing and elevation calibration methods are presented, which are demonstrated to be inevitable in an airborne SAR reconnaissance. It is worthy of remarking that a plane approximation is introduced for geographical coordinates, hence, avoiding the imaging area being very large. However, this constraint is weaker than the constraint of RTK GPS system which allows a largest working in a scope of only 20 km. If RTK GPS works on a large range mode via GPRS net, the measurement error will be increased faster than the algorithm locating error. So this constraint remains weaker than the RTK GPS system. If there is some set measuring the platform attitude on real-time, the algorithm will be more effective and simple. As the back-projection algorithm, the computation burden is somewhat heavy that points to the need of fast algorithms to be exploited in future.

REFERENCES

Arai C and Shikada M. 2001. Research on real-time revision of base map using remote sensing and RTK-GPS. Proceedings IGARSS'01: 2463–2465

Caves R G, Harley P J and Quegab S. 1991. Registering SAR images to digital map data using a template matching technique. Proceddings IGARSS'91: 1429–1431

Earle M D, Brown M R, Shih H H, Sprenke J J, Collier W and Crump D R. 2005. GPS-tracked buoy for hydrographic survey applications. OCEANS, Proceedings of MTS/IEEE.: 1263–1267

Eineder M and Adam N. 2005. A maximum-likelihood estimator to simultaneously unwrap, geocode, and fuse SAR interferograms from different viewing geometries into one digital elevation model. IEEE Trans on GRS, **43**(1): 24–36

He R and Wang Y. 2006. Automatic SAR image coarse registration based on geographical coordinates parameter. *Hunan Daxue Xuebao/Journal of Hunan University Natural Sciences*, **33**: 59–62

Hong S H, Jung H S, Won J S and Kim H G. 2004. Extraction of ground control points (GCPs) from synthetic aperture radar image using DEM. Proceedings IGARSS'04, Seoul, South Korea: 4223–4226

Kirk J C Jr. 1975. Motion compensation for synthetic aperture Radar. *Ieee Transactions on Aerospace and Electronic Systems*: 338–348

Kwok R, Culander J C and Pang S S. 1987. Rectification of terrain induced distortions in radar imagery. *Photogrammetric Engineering and Remote Sensing*, 53

Luojus K P, Pulliainen J T, Blasco Cutrona A, Metsamaki, S J and Hallikainen M T. 2009. Comparison of SAR-based snow-covered area estimation methods for the boreal forest zone. *IEEE Geoscience and Remote Sensing Letters*, (6):403–407

Noack W, Popella A and Schreier G. 1987. Knowledge-based SAR processing and geocoding: the elementary components of the German processing and archiving facility for high throughput and high-precision processing of ERS-1SAR data. *IEEE Transactions on Geoscience and Remote Sensing*, GE–25

Rau R and McClellan J H. 2000. Analytic models and postprocessing techniques for UWB SAR. *IEEE Transactions on Aerospace and Electronic Systems*, 36(4): 1058–1074

Sansosti E, Scheiber R, Fornaro G, Tesauro M, Lanari R and Moreira A. 1997. On the motion compensation and geocoding of airborne interferometric SAR data. Geoscience and Remote Sensing, IGARSS '97. Remote Sensing - A Scientific Vision for Sustainable Development., 1997 IEEE International: 451–453

Ulander L M H. 1996. Radiometric slope correction of synthetic-aperture Radar images. *IEEE Trans on GRS*, 34(5): 1115–1122

Yang M and Lo C F. 2000. Real-time kinematic GPS positioning for centimeter level ocean surface monitoring. *Proceedings National Science Council ROC*(*A*), 24(1): 79–85

Yu J X, Xiao D Y, Jiang L D and Guo R. 2007. Approach for geo-location with unmanned aerial vehicle. *Opto-Electronic Engineering*, 2007, **34(**7): 493–500

Zhang F, Xu M., Xia Z, Wan Z, Li K. and Li X. 2009. Forest mapping using bi-aspect polarimetric SAR data in southwest China. In, *MIPPR 2009-Multispectral Image Acquisition and Processing*: *6th International Symposium on Multispectral Image Processing and Pattern Recognition*, *October 30*, *2009 - November 1*, *2009* (p. Natl. Lab. Multi-spectral Inf. Process. Technol.; Huazhong University of Science and Technology; National Natural Science Foundation of China; China Three Gorges University). Yichang, China: SPIE

后向投影算法的地理坐标系下的合成孔径雷达成像

李杨寰，金添，宋千，周智敏

国防科技大学电子科学与工程学院，湖南 长沙 410073

摘 要：传统的机载合成孔径雷达(SAR)一般依赖于GPS/INS组合系统补偿平台的运动误差，并获得高分辨率的图像。GPS获取的地理坐标(即经度，纬度和高度)需要转换为本地的直角坐标，原始雷达数据在这个直角坐标系下才能引入成像及运动补偿算法进行处理，并获得本地直角坐标系下的图像。这种图像是通过局部坐标描述的，对于其他部门是不通用的，因为其他部门需要的是经过全球地理坐标标绘的图像。本文提出了一种由后向投影算法BP(Back Projection)引出的新的SAR成像算法，它直接在地理坐标下处理，可避免坐标转换的过程。而且生成德图像像素均和地理坐标一一对应，能够很方便地被情报或其他部门使用。而且在仿真试验以及外场试验中，证明了本文算法和常规BP算法成像效果是相当的。

关键词：合成孔径雷达，运动补偿，地理坐标系，坐标转换，高程校正

中图分类号：TP722.6 **文献标志码**：A

引用格式：李杨寰，金添，宋千，周智敏. 2011. 后向投影算法的地理坐标系下的合成孔径雷达成像. 遥感学报，**15**(4)：680–686
Li Y H, Jin T, Song Q and Zhou Z M. 2011. A novel SAR imaging method under geographical coordinates. *Journal of Remote Sensing*, **15**(4): 680–686